

Transient Growth Before Coupled-Mode Flutter

P. J. Schmid¹

E. de Langre

Laboratoire d'Hydrodynamique (LadHyX),
Ecole Polytechnique,
F-91128 Palaiseau, France

Transient growth of energy is known to occur even in stable dynamical systems due to the non-normality of the underlying linear operator. This has been the object of growing attention in the field of hydrodynamic stability, where linearly stable flows may be found to be strongly nonlinearly unstable as a consequence of transient growth. We apply these concepts to the generic case of coupled-mode flutter, which is a mechanism with important applications in the field of fluid-structure interactions. Using numerical and analytical approaches on a simple system with two degrees-of-freedom and antisymmetric coupling we show that the energy of such a system may grow by a factor of more than 10, before the threshold of coupled-mode flutter is crossed. This growth is a simple consequence of the nonorthogonality of modes arising from the nonconservative forces. These general results are then applied to three cases in the field of flow-induced vibrations: (a) panel flutter (two-degrees-of-freedom model, as used by Dowell) (b) follower force (two-degrees-of-freedom model, as used by Bamberger) and (c) fluid-conveying pipes (two-degree-of-freedom model, as used by Benjamin and Paidoussis) for different mass ratios. For these three cases we show that the magnitude of transient growth of mechanical energy before the onset of coupled-mode flutter is substantial enough to cause a significant discrepancy between the apparent threshold of instability and the one predicted by linear stability theory. [DOI: 10.1115/1.1631591]

1 Introduction

Flow-induced vibration phenomena are a ubiquitous feature in numerous engineering applications ranging from buffeting of airfoils to deformation of building structures and bridges under wind loads. In most cases, these vibrations are undesirable, causing material fatigue at best and catastrophic failure at worst. It is thus not surprising that a substantial body of literature is devoted to the analysis and control of flow-induced instabilities. Low-dimensional models are often used to approximate prohibitively complex systems, and the critical parameters for the onset of flutter are computed for a moderate number of degrees-of-freedom. The analysis follows a typical modal approach where the temporal motion of the structure is assumed to behave exponentially in time. In the very common mechanism of coupled-mode flutter two (or more) purely oscillatory states merge and produce exponentially growing (and decaying) motion. For parameter values below this critical one, it is believed that stable motion prevails.

A similar argument has been used for the onset of transition to turbulence: As exponentially growing solutions of the linearized fluids equations are encountered, the transition to turbulent fluid motion is expected. In recent years, however, it has been discovered that short-term instabilities are present even at subcritical parameter values, and that these type of instabilities are a consequence of the nature of the underlying stability equations (see, e.g., [1–4]).

The equations governing many cases of fluid-structure interactions are also of this type, and it therefore appears likely that the governing equations support transiently growing solutions for parameter values below the critical one for the onset of coupled-

mode flutter. If this transient growth is sufficiently large, finite-amplitude effects can be triggered even though infinitesimal motion is asymptotically stable.

It is the goal of this study to explore the potential of short-term energy growth at subcritical conditions for simple two-degrees-of-freedom approximations to technologically relevant configurations.

The organization of the paper is as follows. We will first consider a simple undamped two-degrees-of-freedom model of coupled-mode flutter and establish the mathematical framework for stability calculations. Modal and nonmodal stability will be considered, and asymptotic scalings as well as upper bounds on disturbance growth will be presented. Effects of damping on the stability characteristics will be treated as well. Three classical applications then follow, namely, panel flutter, [5], follower-force, [6], and fluid-conveying pipes, [7], which will further exemplify the techniques of the previous sections. Summarizing comments conclude this paper.

2 Theoretical Framework

2.1 General Undamped Two-Degrees-of-Freedom System

Many problems involving fluid-structure interactions can be modeled by a coupled system of oscillators of the form

$$\ddot{x} + x = ay \quad (1a)$$

$$\ddot{y} + \Omega^2 y = -ax \quad (1b)$$

describing the temporal evolution of the two degrees-of-freedom x and y . The left-hand side describes harmonic oscillators of frequencies 1 and Ω , while the right-hand side accounts for the coupling of the two oscillators with a as the coupling coefficient. Systems of this form often arise when equations governing the continuous deformation of flexible structures are approximated by a model capturing the two modes of deflection. This typically applies to problems such as flutter of flexible airfoils, fluidelastic instability of tube arrays in cross flow or unstable whirl of rotating shafts in confined fluids (see, for instance, [5,8,9]).

Traditional stability analysis of the above system is straightforward and leads to a critical coupling coefficient a_c of

¹Permanent address: Department of Applied Mathematics, University of Washington, Box 352420, Seattle, WA 98195-2420.

Contributed by the Applied Mechanics Division of THE AMERICAN SOCIETY OF MECHANICAL ENGINEERS for publication in the ASME JOURNAL OF APPLIED MECHANICS. Manuscript received by the ASME Applied Mechanics Division, August 13, 2002; final revision, June 12, 2003. Associate Editor: A. A. Ferri. Discussion on the paper should be addressed to the Editor, Prof. Robert M. McMeeking, Department of Mechanical and Environmental Engineering, University of California—Santa Barbara, Santa Barbara, CA 93106-5070, and will be accepted until four months after final publication of the paper itself in the ASME JOURNAL OF APPLIED MECHANICS.

$$a_c = \frac{\Omega^2 - 1}{2}. \quad (2)$$

For two oscillators with a supercritical coupling coefficient exponentially growing solutions are encountered. For coupling coefficients below the critical one, we observe purely oscillatory behavior. The above critical coupling coefficient is a widely used and accepted tool for determining the onset of unstable motion. It is commonly believed that for coupling coefficients below the critical one no amplification of infinitesimal disturbances is possible.

2.2 Transient Amplification of Disturbance Energy. The goal of this manuscript is to explore the potential for short-term linear instabilities in the absence of exponentially growing solutions. To this end we treat the above system of equations as a general initial value problem of the form

$$\frac{d}{dt} \begin{pmatrix} x \\ \dot{x} \\ y \\ \dot{y} \end{pmatrix} = \begin{pmatrix} 0 & 1 & 0 & 0 \\ -1 & 0 & a & 0 \\ 0 & 0 & 0 & 1 \\ -a & 0 & -\Omega^2 & 0 \end{pmatrix} \begin{pmatrix} x \\ \dot{x} \\ y \\ \dot{y} \end{pmatrix} \quad \text{or} \quad \frac{d}{dt} \mathbf{q} = \mathbf{A}\mathbf{q}. \quad (3)$$

The formal solution of this initial value problem can be written in terms of the matrix exponential of \mathbf{A} . We obtain

$$\mathbf{q}(t) = \exp(t\mathbf{A})\mathbf{q}_0 \quad (4)$$

with \mathbf{q}_0 as the vector of initial conditions x_0 , \dot{x}_0 , y_0 , and \dot{y}_0 . Using this formulation, we wish to compute the amplification of disturbances by determining the ratio of the disturbance energy at a given time t to the initial energy of a general perturbation. Maximizing this ratio over all possible initial conditions results in the largest possible amplification of initial perturbations over a time span $[0, t]$. Mathematically, we define the largest possible energy amplification $G(t)$ as

$$G(t) = \max_{\mathbf{q}_0} \frac{E(t)}{E(0)} = \max_{\mathbf{q}_0} \frac{\|\mathbf{q}(t)\|^2}{\|\mathbf{q}_0\|^2} = \max_{\mathbf{q}_0} \frac{\|\exp(t\mathbf{A})\mathbf{q}_0\|^2}{\|\mathbf{q}_0\|^2} = \|\exp(t\mathbf{A})\|^2 \quad (5)$$

where we have assumed that taking the norm of the state vector \mathbf{q} is equivalent to computing the energy of the state vector. We therefore define

$$\|\mathbf{q}\|^2 = x^2 + \dot{x}^2 + \Omega^2 y^2 + \dot{y}^2 \quad (6)$$

which is easily related to the standard L_2 -norm $\|\cdot\|_2$ by introducing weight matrices \mathbf{F} according to

$$\|\mathbf{q}\|^2 = \|\mathbf{F}\mathbf{q}\|_2^2 \quad \mathbf{F} = \begin{pmatrix} 1 & 0 & 0 & 0 \\ 0 & 1 & 0 & 0 \\ 0 & 0 & \Omega & 0 \\ 0 & 0 & 0 & 1 \end{pmatrix}. \quad (7)$$

Reformulating the energy amplification $G(t)$ in terms of the L_2 -norm results in

$$G(t) = \|\mathbf{F} \exp(t\mathbf{A}) \mathbf{F}^{-1}\|_2^2. \quad (8)$$

It is often desirable to bound the maximum amplification of energy. Using the definition of the energy amplification it is straightforward to derive lower and upper bounds as follows:

$$\exp(2\lambda t) \leq G(t) = \|\mathbf{S} \exp(\Lambda t) \mathbf{S}^{-1}\|^2 \leq \kappa^2(\mathbf{S}) \exp(2\lambda t) \quad (9)$$

where λ is the real part of the least stable eigenvalue of \mathbf{A} , and \mathbf{S} denotes the 4×4 matrix of normalized eigenvectors of \mathbf{A} . The symbol

$$\kappa(\mathbf{S}) \equiv \|\mathbf{S}\| \|\mathbf{S}^{-1}\| \quad (10)$$

stands for the condition number of \mathbf{S} , and Λ is a diagonal 4×4 matrix containing the eigenvalues of \mathbf{A} .

We notice the following relation. For systems with $\kappa(\mathbf{S}) = 1$ the upper and lower bound coincide, and the temporal evolution of G is entirely governed by the real part of the least stable eigenvalue. Systems with $\kappa(\mathbf{S}) = 1$ are known as *normal* systems. On the other hand, if $\kappa(\mathbf{S})$ is larger than 1, the discrepancy between lower and upper bound allows for short-term effects before the exponential behavior governed by λ prevails as $t \rightarrow \infty$. Systems with $\kappa(\mathbf{S}) > 1$ are categorized as *non-normal* systems. Non-normal systems have a set of nonorthogonal eigenvectors and the source of short-term energy growth lies in this nonorthogonality of the system's eigenvectors. Even under subcritical conditions, i.e., for coupling coefficients below the critical one, a nonorthogonal superposition of exponentially decaying eigensolutions can lead to substantial disturbance growth.

2.3 Asymptotic Scalings. To further probe the solution behavior as we approach the critical coupling coefficient a_c we Laplace transform the governing equations to obtain

$$(p^2 + 1)X - aY = px_0 + \dot{x}_0 \quad (11a)$$

$$(p^2 + \Omega^2)Y - aX = py_0 + \dot{y}_0 \quad (11b)$$

with $X(p)$ and $Y(p)$ as the Laplace transform of the dependent variables $x(t)$ and $y(t)$, respectively. Solving for $X(p)$ we obtain the expression

$$X(p) = \frac{1}{(p^2 + 1)(p^2 + \Omega^2) + a^2} [A + pB + p^2C + p^3D] \quad (12)$$

with A , B , C , and D determined from the initial conditions. An analogous expression can be derived for $Y(p)$. After inversion of the Laplace transform we get the following expression for the variable $x(t)$:

$$x(t) = \frac{1}{2a_c \sqrt{1 - (a/a_c)^2}} [A' \cos \alpha t + B' \sin \alpha t + C' \cos \beta t + D' \sin \beta t] \quad (13)$$

where

$$\alpha^2, \beta^2 = \frac{1}{2} (1 + \Omega^2 \pm \sqrt{(\Omega^2 - 1)^2 - 4a^2}) \quad (14)$$

and A' , B' , C' , and D' depend on initial conditions. This last expression yields the behavior of $x(t)$ as the critical coupling coefficient is approached. We obtain

$$x(t) \sim \frac{1}{\sqrt{1 - (a/a_c)^2}}. \quad (15)$$

The same holds true for $\dot{x}(t)$, $y(t)$, and $\dot{y}(t)$. Consequently, the energy E of the coupled oscillators is expected to behave as

$$E \sim \frac{1}{1 - (a/a_c)^2} \quad (16)$$

as the stability boundary is approached, when time is fixed.

2.4 Numerical Results. The quantity $G(t)$, computed from Eq. (8), represents the maximum possible energy amplification, which for each instant in time is optimized over all possible initial conditions of unit energy, as is apparent from Eq. (5). The specific initial condition that achieves an amplification of $G(t)$ may be different for different times, and $G(t)$ should be thought of as the envelope of the energy evolution of individual initial conditions of unit energy. The energy amplification $G(t)$ for the undamped general system with $\Omega^2 = 1.1$ and $a/a_c = 0.9$ is shown in Fig. 1(a) together with the energy evolution of four randomly chosen initial conditions of unit energy. We notice an amplification of energy of nearly twenty times the initial energy after approximately 150

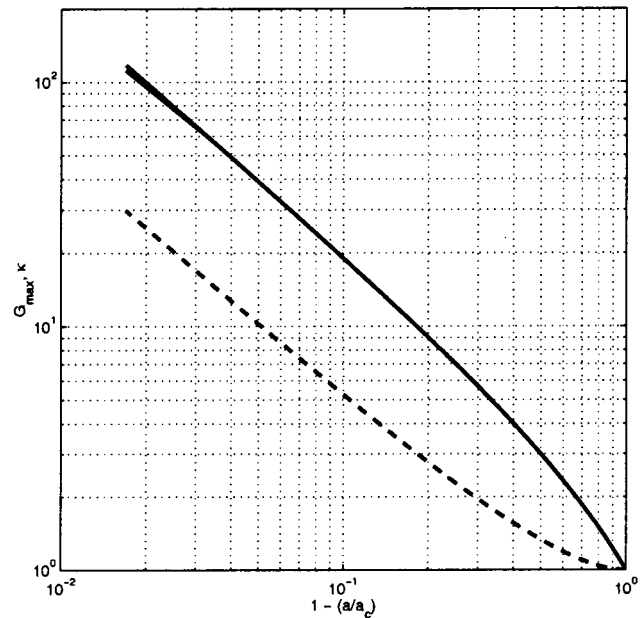
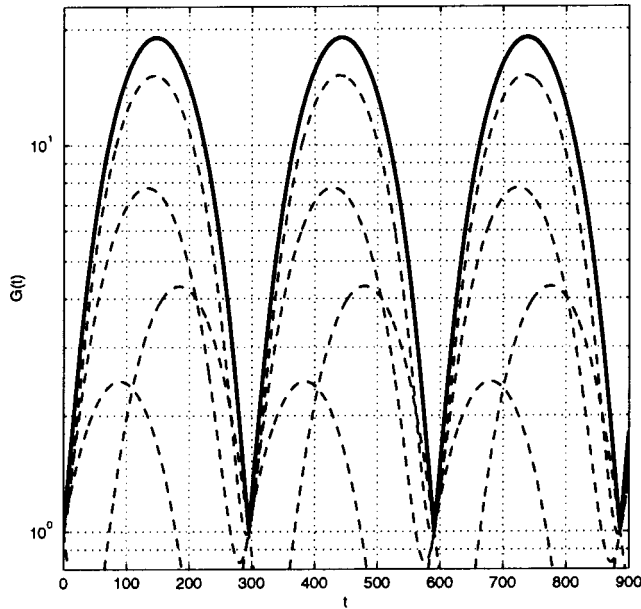


Fig. 1 General undamped system with $\Omega^2=1.1$ and $a/a_c=0.9$. Optimal energy amplification versus time (top, solid line) and energy amplification for four random initial conditions of unit energy (top, dashed lines). Maximum energy amplification versus the coupling coefficient (bottom). The dashed curve (bottom) represents the function $1/(1-(a/a_c)^2)$. The continuous curve (bottom) represents both the maximum of $G(t)$ over time and the upper bound given in Eq. (9).

time units. We like to emphasize that this amplification occurs at a value of the coupling coefficient that is below the critical one for the onset of couple-mode flutter. As the critical coupling coefficient for this particular frequency ratio Ω is approached we obtain an even larger transient amplification of initial energy, as depicted in Fig. 1(b). The asymptotic behavior given by (16) is included as the dashed curve. As the critical coupling coefficient is approached, the maximum transient amplification of energy $G_{\max} \equiv \max_t G(t)$ follows the correct asymptotic behavior.

The transient amplification of disturbance energy prevails also for a significantly larger frequency ratio. Figure 2(a) shows the temporal evolution of G for a frequency ratio of $\Omega^2=10$. Again,

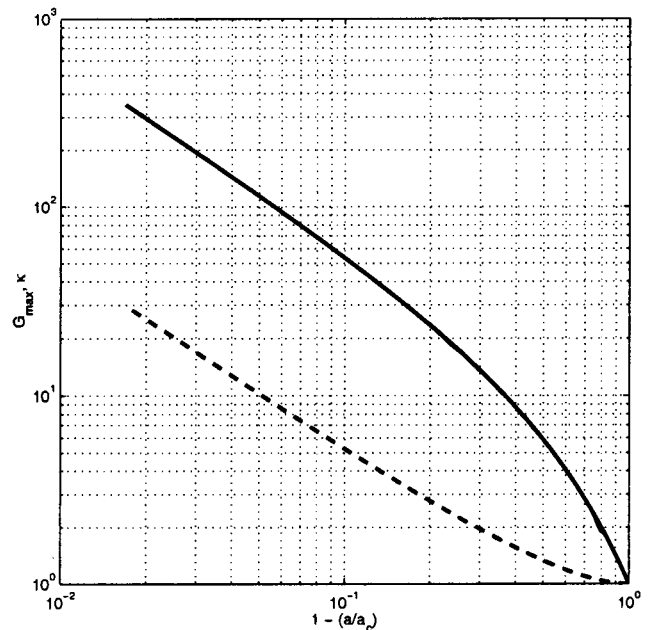
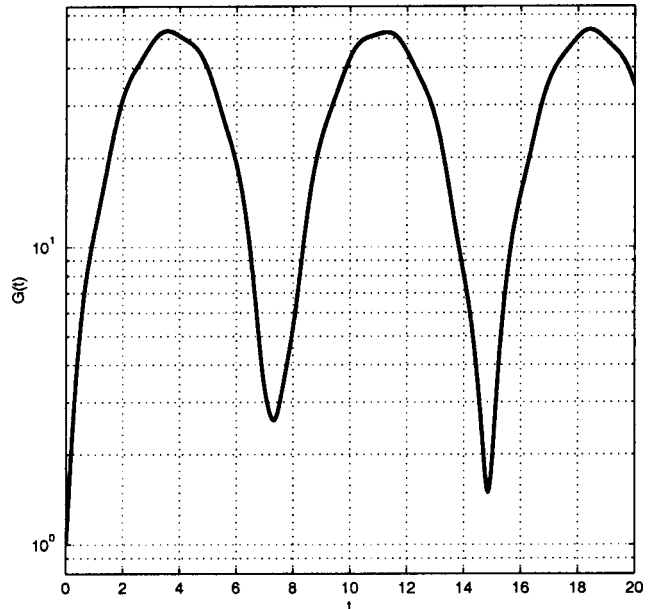


Fig. 2 General undamped system with $\Omega^2=10$ and $a/a_c=0.9$. Energy amplification versus time (top) and maximum energy amplification versus the coupling coefficient (bottom). The dashed curve represents the function $1/(1-(a/a_c)^2)$. The continuous curve represents both the maximum of $G(t)$ over time and the upper bound given in Eq. (9).

we observe a short-term amplification of initial energy of up to fifty times. The behavior of G_{\max} as the critical coupling coefficient is approached is displayed in Fig. 2(b) together with the asymptotic behavior (16).

2.5 Effects of Damping. Damping is a naturally occurring effect in many fluid-structure systems that has to be accounted for or modeled when analyzing the onset of coupled-mode flutter. In this paper, we are mainly interested how additional damping terms modify the observations we made in the previous section. We again start by analyzing a simple two-degrees-of-freedom model, but add a damping term proportional to the velocity. We get

$$\ddot{x} + b\dot{x} + x = ay \quad (17a)$$

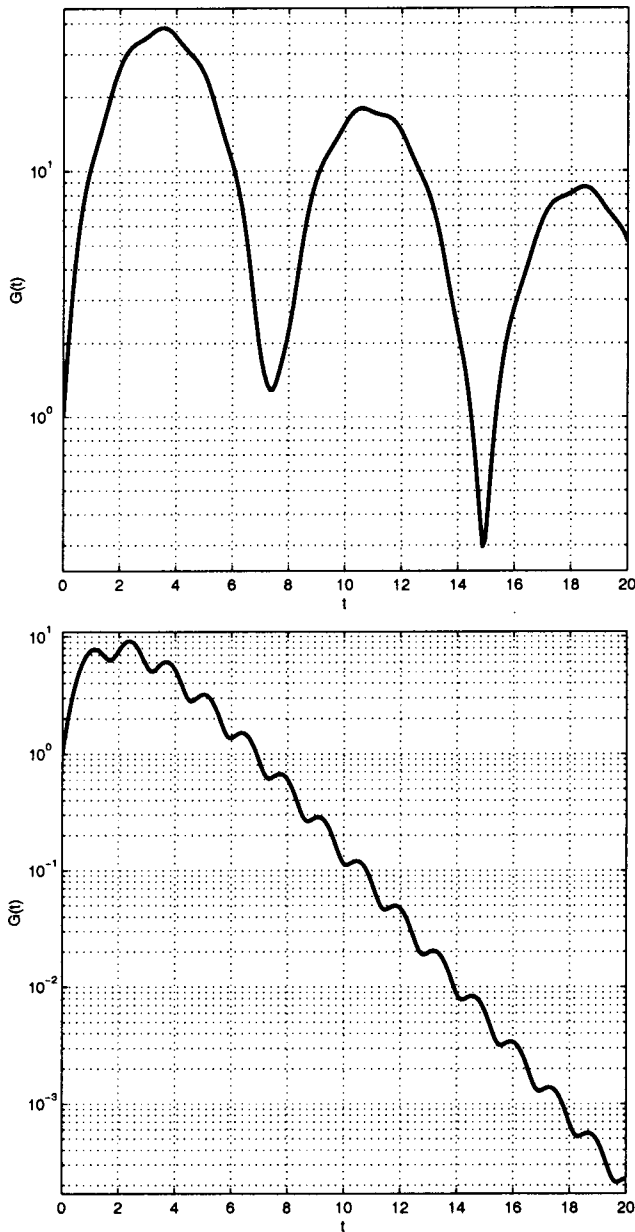


Fig. 3 General damped system with $\Omega^2=10$ and $a/a_c=0.9$. For damping a coefficient of $b=0.1$, (top) and a damping coefficient of $b=1$ (bottom).

$$\ddot{y} + b\dot{y} + \Omega^2 y = -ax \quad (17b)$$

with b as the damping coefficient. Traditional stability analysis of this problem follows along the same lines as for the undamped case. Applying a Laplace transform to the initial value problem results in the relation

$$\det \begin{vmatrix} p^2 + bp + 1 & -a \\ a & p^2 + bp + \Omega^2 \end{vmatrix} = 0 \quad (18)$$

from which—via Routh's criterion—we obtain a value for the critical coupling coefficient for the onset of flutter motion:

$$a_c = a_c^0 \sqrt{1 - 2b^2 \frac{\Omega^2 + 1}{(\Omega^2 - 1)^2}} \quad (19)$$

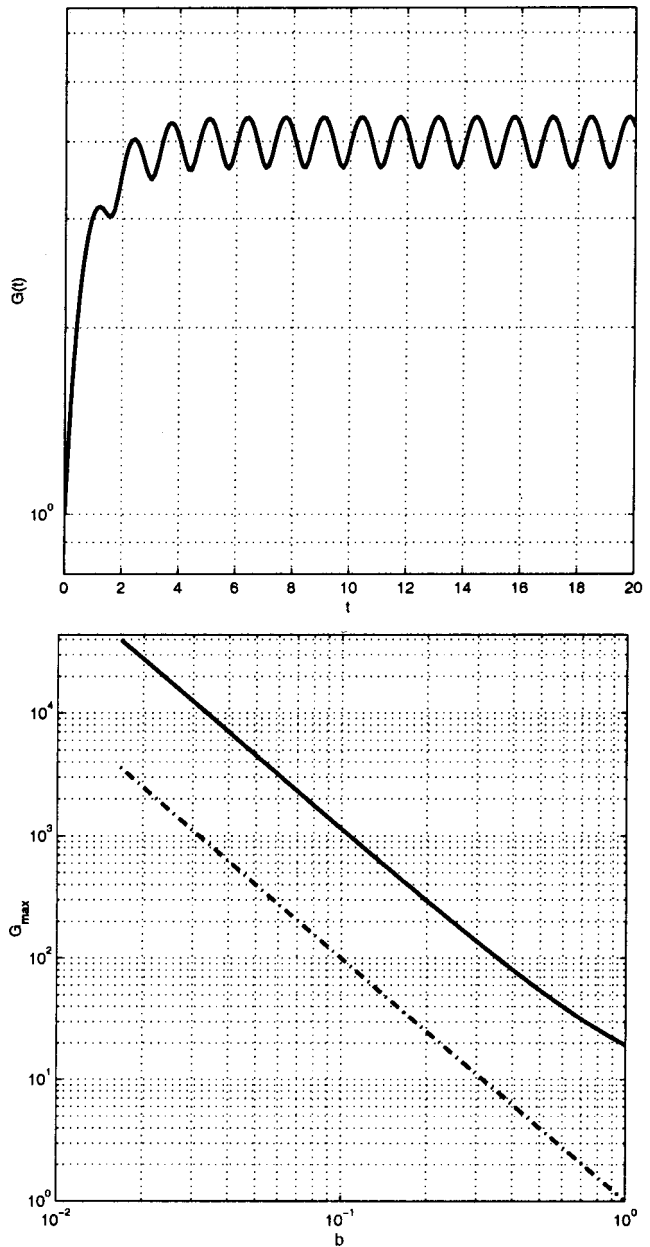


Fig. 4 General damped system with $\Omega^2=10$ at criticality. Energy amplification versus time for $b=1$ (top), and maximum energy amplification versus damping coefficient (bottom). The dashed curve represents the asymptotic behavior $\sim 1/b^2$.

The above formula describes the modification of the critical coupling coefficient when a velocity-dependent damping term is introduced into the governing equations.

We are of course also interested in the effects of damping on the potential for transient amplification at subcritical values of the coupling constant. Modifying the system matrix \mathbf{A} to account for the additional damping terms, we compute the amplification of disturbance energy $G(t)$ as in the previous section.

The results in Fig. 3 demonstrate that the additional damping terms exert a rather substantial—but not surprising—influence on the long-term behavior. The short-term amplification of energy, on the other hand, is only mildly influenced by damping. We still observe an energy amplification of approximately forty times the initial energy for a damping coefficient of $b=0.1$, and even for an excessively large damping of $b=1$ we obtain an increase in energy of nearly one order of magnitude before strong decay sets in

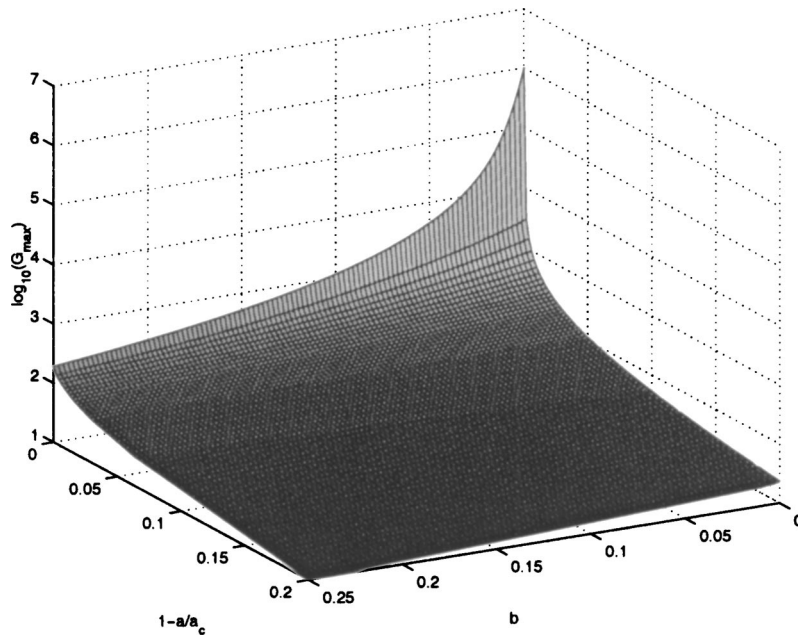


Fig. 5 Maximum energy amplification as a function of coupling and damping coefficient for the general damped system at $\Omega^2=10$

(see Fig. 3). As the critical coupling parameter (19) is approached, an oscillatory state is reached for $G(t)$ with a maximum amplification of more than forty times the initial energy (see Fig. 4(a)).

A simple analysis shows that at the onset of instability, i.e., for $a=a_c$, the solution to the damped system behaves like

$$x \sim e^{-bt}(\cos at + t \cos at + \dots) \quad (20)$$

and similarly for the y -component. For this solution behavior, the maximum of the energy amplification is found to occur at $t \approx 1/b$ and the maximum transient growth scales like $G_{\max} \sim 1/b^2$. This scaling is verified by numerical computations with the results shown in Fig. 4(b). The asymptotic scaling is displayed as the dashed curve.

A two-dimensional parameter study of the maximum amplification of initial disturbance energy is depicted in Fig. 5. We observe a substantial amount of maximum transient growth as the stability boundary is approached.

The above analysis describes external damping that acts with equal magnitude on the two degrees-of-freedom. It is a well-known fact (see [10,11]) that a discrepancy between the damping in the equations for x and y can have a stabilizing or destabilizing effect and thus change the critical coupling constant. Following Bolotin [10] and introducing a damping coefficient of b and ηb into the x and y -equation, respectively, the critical coupling coefficient can be derived as

$$a_c = a_c^0 \left(\frac{2\sqrt{\eta}}{1+\eta} \right) \sqrt{1 + b^2 \frac{(1+\eta)\Omega^2 + \eta + \eta^2}{(\Omega^2 - 1)^2}} \quad (21)$$

which represents the generalization of Eq. (19) which is recovered for $\eta=1$. Numerical experiments have revealed that the transient effects observed for $\eta=1$ prevail qualitatively for the more general case once the critical coupling coefficient has been redefined according to Eq. (21).

3 Applications

The strong short-term amplification of initial energy for parameters below the critical ones for the onset of coupled-mode flutter can have significant consequences for the design of systems that exhibit aeroelastic deformations or other fluid-structure phenomena. The above analysis of a simple two-degrees-of-freedom sys-

tem provides the mathematical tools as well as the motivation to investigate more realistic models of fluid-structure interactions for their potential to amplify energy in the subcritical parameter regime. To this end, we concentrate on three classical and well-studied examples of two-degrees-of-freedom systems: (a) panel flutter, (b) follower-force, and (c) fluid-conveying pipes (see Fig. 6 for a sketch of the geometry). For each system we will compute and present the amplification of energy $G(t)$ over a range of governing parameters.

3.1 Panel Flutter. As high-speed flow passes a flat plate with clamped edges, the induced elastic bending in the direction normal to the flow can lead to vibrational instabilities. This type of instabilities is prototypical and very important for many con-

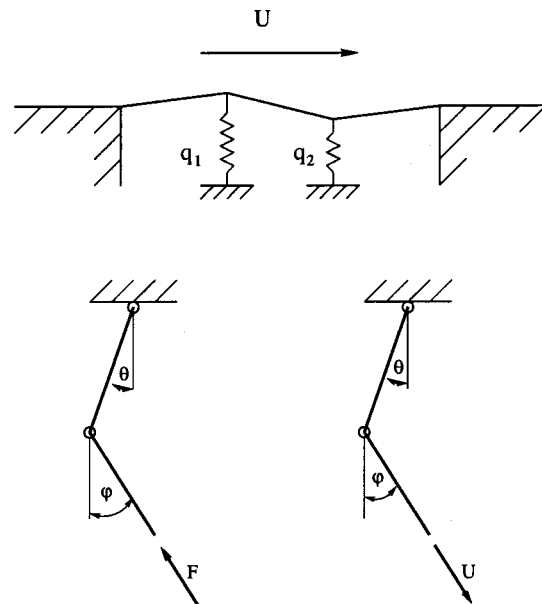


Fig. 6 Geometry sketch for panel flutter (top), follower force (bottom left), and fluid-conveying pipe (bottom right)

figurations in aerospace applications (supersonic flow past an airfoil) and has thus been studied extensively. In this paper we will focus on a highly simplified, yet physically relevant, model which will capture some of the main features of panel flutter instabilities. The model under investigation is taken from Dowell [5]. Three plates of length l and mass m are linked together and supported at each end (see Fig. 6(a)) introducing two degrees-of-freedom for the motion of the system. With q_1 and q_2 as the vertical displacement of the interior nodes, Dowell [5] derives the following set of equations

$$\frac{2}{3}ml\ddot{q}_1 + \frac{ml}{6}\ddot{q}_2 + kq_1 + \frac{\rho_\infty U_\infty^2}{2M_\infty}q_2 = 0 \quad (22a)$$

$$\frac{ml}{6}\ddot{q}_1 + \frac{2}{3}ml\ddot{q}_2 + kq_2 - \frac{\rho_\infty U_\infty^2}{2M_\infty}q_1 = 0 \quad (22b)$$

where k denotes the spring constant, and ρ_∞ , U_∞ , and M_∞ stand for the freestream density, velocity, and Mach number, respectively. Nondimensionalizing the above equations using $\lambda = \rho_\infty U_\infty^2 / 2M_\infty k$ and $\sqrt{m/lk}$ as a characteristic time scale, we obtain

$$\frac{2}{3}\ddot{q}_1 + \frac{1}{6}\ddot{q}_2 + q_1 = -\lambda q_2, \quad (23a)$$

$$\frac{1}{6}\ddot{q}_1 + \frac{2}{3}\ddot{q}_2 + q_2 = \lambda q_1. \quad (23b)$$

We can further simplify the system by introducing new dependent variables defined as $x = \sqrt{5/3}(q_1 + q_2)$ and $y = q_1 - q_2$ which yields

$$\ddot{x} + x = ay \quad (24a)$$

$$\ddot{y} + \Omega^2 y = -ax \quad (24b)$$

with $\Omega^2 = 5/3$ and $a = \sqrt{5/3}\lambda$.

In this form, the reduced system resembles the undamped two-degrees-of-freedom system of the previous section, and we should expect the existence of transient amplification of energy for subcritical coupling coefficients λ . The critical coupling coefficient is $a_c = 1/3$, equivalent to $\lambda_c = 1/\sqrt{15}$ in [5]. Figure 7(a) shows the maximum energy amplification $G(t)$ as a function of time for $a/a_c = 0.9$ or, equivalently, $(U_\infty/U_c)^2 = 0.9$ where U_c is the critical flow velocity. For this choice of parameter we observe an amplification of 20 times the initial energy. As the critical coupling coefficient is approached, we again recover the proper asymptotic scaling (dashed curved) as displayed in Fig. 7(b). These results clearly demonstrate that large disturbance growth is possible even before the coalescence of natural frequencies and, thus, the onset of panel flutter.

3.2 Follower Force. A slightly more complex two-degrees-of-freedom model is sketched in Fig. 6(b) where two hinged rods of length l are subject to a force F acting on the bottom and in the direction of the lower rod. The motion of the two rods is affected by a torsional spring acting at the hinge. The configuration of the rods is described by the angles θ and ϕ measured with respect to the vertical axis. We will follow Bamberger [6] in deriving the system of equations governing the above configuration. Benjamin [7] has studied models of this type and the specific case illustrated in Fig. 6(b) emerges as a particular case of a fluid-conveying pipe for zero mass ratio β and infinite fluid velocity U , but constant $\sqrt{\beta}U$ (see Paidoussis [12]).

According to Bamberger [6], but using the dimensionless parameters of Benjamin [7] for the sake of clarity, the governing equations are given as

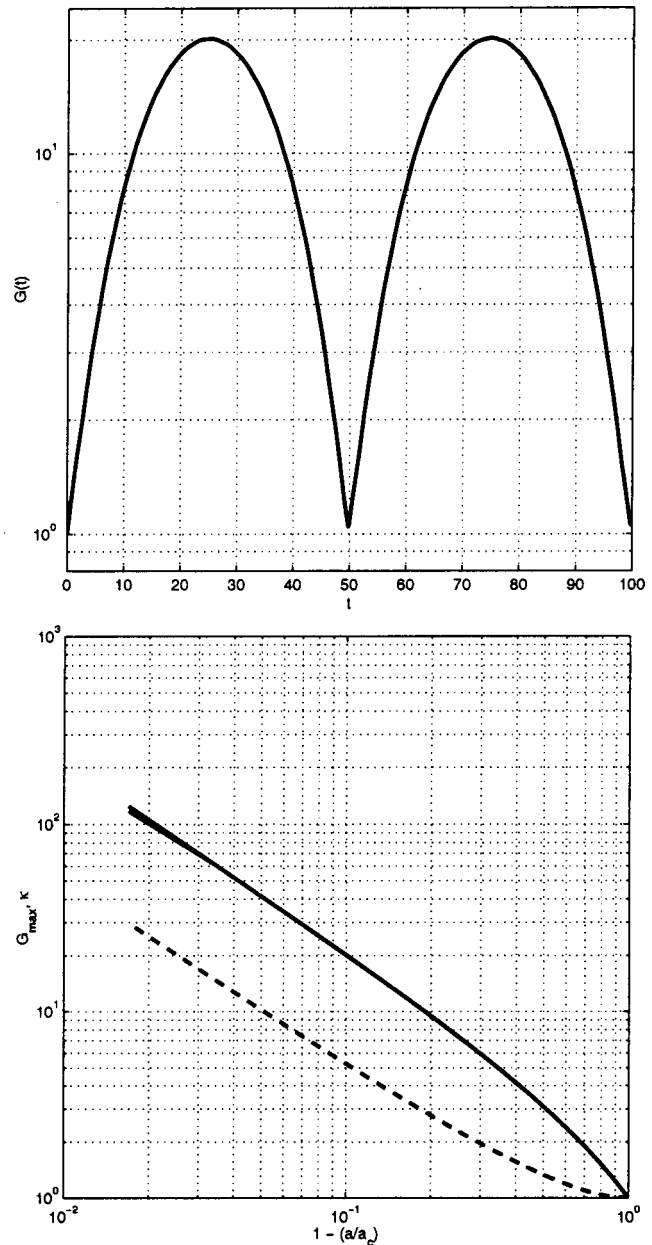


Fig. 7 Energy amplification for undamped panel flutter with $a/a_c = 0.9$ versus time (top), maximum energy amplification versus coupling coefficient (bottom). The dashed curve represents the asymptotic behavior $1/(1 - (a/a_c)^2)$. The continuous curve represents both the maximum of $G(t)$ over time and the upper bound given in Eq. (9).

$$\begin{bmatrix} 4 & 3/2 \\ 3/2 & 1 \end{bmatrix} \begin{bmatrix} \ddot{\theta} \\ \ddot{\phi} \end{bmatrix} + \begin{bmatrix} 2 & -1 \\ -1 & 1 \end{bmatrix} \begin{bmatrix} \theta \\ \phi \end{bmatrix} = a \begin{bmatrix} 1 & -1 \\ 0 & 0 \end{bmatrix} \begin{bmatrix} \theta \\ \phi \end{bmatrix} \quad (25)$$

with $a = F/kl$ as the coupling coefficient.

At a value of $a = 0.1$, we determine the two natural frequencies of the system as $\omega_1 = 0.337$ and $\omega_2 = 2.243$ which results in the square of the frequency ratio $\Omega^2 = 44.4$. Increasing the parameter a beyond this critical point, which Bamberger [6] determined as $a_c = 2.54$, exponentially growing solutions are encountered. Again, we wish to probe the possibility and amount of short-term energy growth for parameter values a below the critical one.

In order to use the formalism introduced in this paper, we define the system matrix \mathbf{A} in (3) as

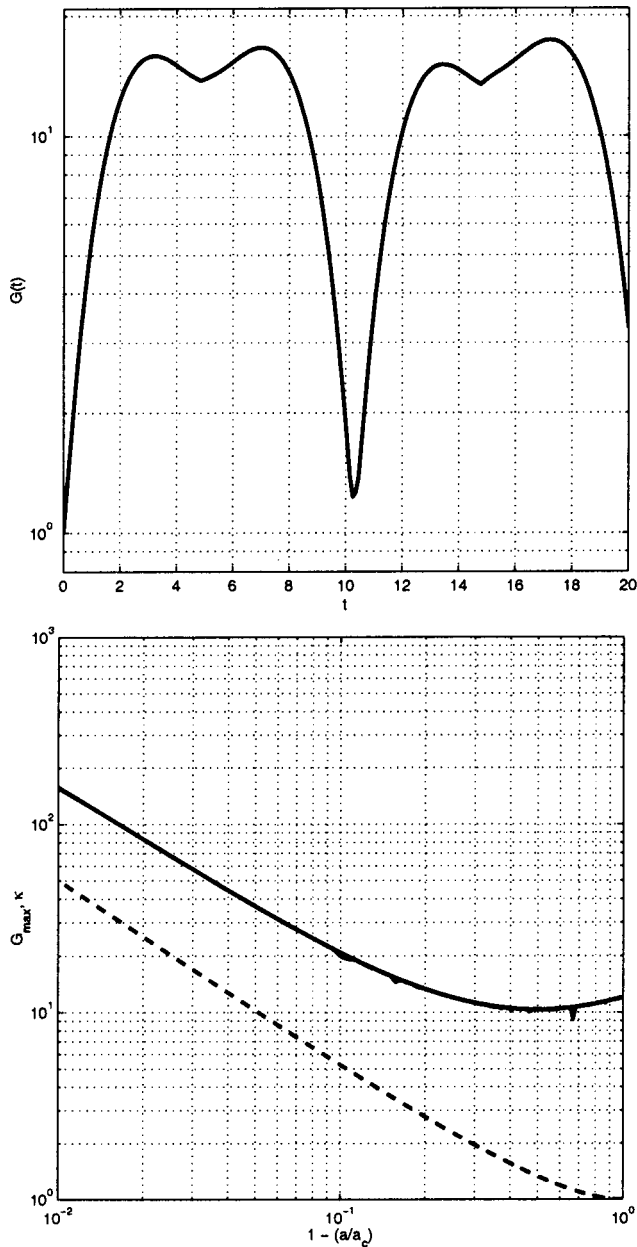


Fig. 8 Energy amplification for undamped follower force problem with $a/a_c=0.9$ versus time (top), maximum energy amplification versus coupling coefficient (bottom). The dashed curve represents the asymptotic behavior $1/(1-(a/a_c)^2)$. The continuous curve represents both the maximum of $G(t)$ over time and the upper bound given in Eq. (9).

$$A = \begin{pmatrix} 1 & 0 & 0 & 0 \\ 0 & 4 & 0 & 3/2 \\ 0 & 0 & 1 & 0 \\ 0 & 3/2 & 0 & 1 \end{pmatrix}^{-1} \begin{pmatrix} 0 & 1 & 0 & 0 \\ (a-2) & 0 & (1-a) & 0 \\ 0 & 0 & 0 & 1 \\ 1 & 0 & -1 & 0 \end{pmatrix} \quad (26)$$

Alternatively, using different dependent variables the governing equations can be rewritten in the form

$$\ddot{x} + x = \alpha(y - \xi x) \quad (27a)$$

$$\ddot{y} + \Omega^2 y = -\alpha(x + \zeta y) \quad (27b)$$

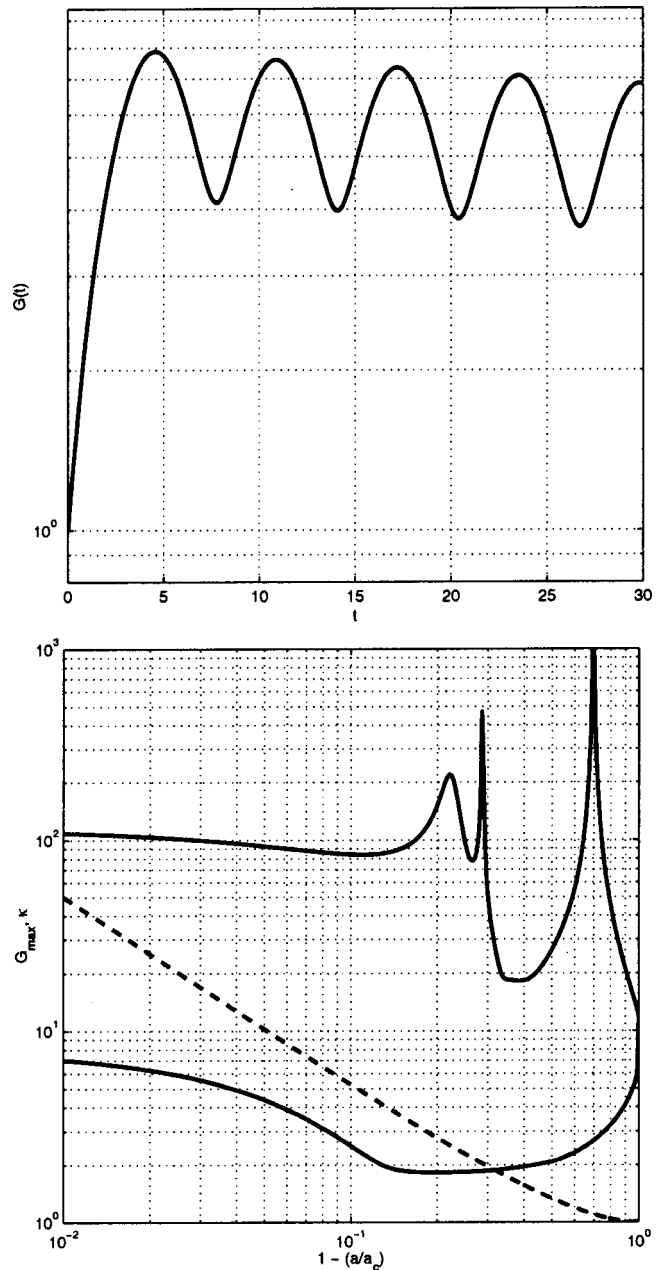


Fig. 9 Energy amplification for the fluid-conveying pipe problem with $a/a_c=0.999$ versus time (top), maximum energy amplification versus coupling coefficient (bottom). The dashed curve represents the asymptotic behavior $1/(1-(a/a_c)^2)$. The top curve represents the square of the condition number of the eigenvector matrix and acts as an upper bound on the maximum energy amplification.

with $\Omega^2=44.4$ and α proportional to a . Strictly speaking, due to the different coupling term, the above system does not resemble the general undamped system introduced previously. Nevertheless, the results of our analysis are similar to the ones found for Eq. (3).

Indeed, computing the maximum energy amplification reveals transient growth of more than one order of magnitude even though the coupling coefficient is only 90 percent of the critical one (see Fig. 8(a)). The asymptotic scaling as criticality is approached is once again confirmed numerically (Fig. 8(b)).

3.3 Fluid-Conveying Pipe. As our last example we consider the instability of an articulated fluid-conveying pipe (see Fig.

6(c)). Benjamin [7] and Païdoussis [12] have studied the stability and dynamics of this configuration in great depth. We will closely follow their derivation, nondimensionalization and choice of governing parameters resulting in the following set of governing equations:

$$\begin{aligned} & \begin{bmatrix} 4 & 3/2 \\ 3/2 & 1 \end{bmatrix} \begin{bmatrix} \ddot{\theta} \\ \ddot{\phi} \end{bmatrix} + \begin{bmatrix} 2 & -1 \\ -1 & 1 \end{bmatrix} \begin{bmatrix} \dot{\theta} \\ \dot{\phi} \end{bmatrix} \\ & = -3\sqrt{\beta}v \begin{bmatrix} 1 & 2 \\ 0 & 1 \end{bmatrix} \begin{bmatrix} \dot{\theta} \\ \dot{\phi} \end{bmatrix} - 3v^2 \begin{bmatrix} -1 & 1 \\ 0 & 0 \end{bmatrix} \begin{bmatrix} \theta \\ \phi \end{bmatrix} \quad (28) \end{aligned}$$

with $\beta = m_{fluid}/(m_{pipe} + m_{fluid})$ as the mass ratio and v as the nondimensional fluid velocity. We recover the follower-force problem discussed in the previous section for the case $\beta = 0$.

We again define the system matrix \mathbf{A} in (3) as

$$\mathbf{A} = \begin{pmatrix} 1 & 0 & 0 & 0 \\ 0 & 4 & 0 & 3/2 \\ 0 & 0 & 1 & 0 \\ 0 & 3/2 & 0 & 1 \end{pmatrix}^{-1} \begin{pmatrix} 0 & 1 & 0 & 0 \\ (a-2) & -b & (1-a) & -2b \\ 0 & 0 & 0 & 1 \\ 1 & 0 & -1 & -b \end{pmatrix} \quad (29)$$

where $a = 3v^2$ and $b = 3\sqrt{\beta}v$.

Evaluating the maximum energy growth versus time we notice that the amplification is somewhat smaller than in the previous cases with energy growth of only about eight times the initial energy (Fig. 9(a)) for a coupling coefficient $a = 0.999a_c$. In addition, flow-induced damping effects are clearly present acting mainly on the second mode. Owing to this damping the maximum amplification of initial energy does not follow the asymptotic behavior (16) as the critical coupling coefficient is approached (see Fig. 9(b)). However, in the limit of $\beta \rightarrow 0$ we recover the correct asymptotic behavior of G_{max} as $a \rightarrow a_c$.

Included in Fig. 9(b) is the upper bound based on the condition number $\kappa(\mathbf{S})$ as introduced in (9). Although the condition number provides a simple estimate, the actual maximum energy growth is one order of magnitude smaller. In all previous cases, the estimate of maximum energy growth (9) based on the condition number was within plotting accuracy of the computed G_{max} .

4 Conclusions

We studied simple two-degrees-of-freedom systems arising in a variety of applications and investigated the potential for short-term amplification of initial energy under subcritical conditions. This amplification is due to the nonorthogonal superposition of modal solutions which in turn is a consequence of the non-normal nature of the underlying system matrix. The maximum achievable growth can be significant and scales like $\sim 1/(1 - (a/a_c)^2)$ as the critical coupling coefficient a_c is approached in the absence of damping. For damped systems, the maximum growth scales inversely to the square of the damping constant.

Since the nonorthogonality of the leading eigenfunctions is preserved as more modes are included in an attempt to model the continuous system, we expect transient amplification of energy in discrete models of high degrees-of-freedom as well as in continuous models. In fact, the inclusion of more nonorthogonal modes

may give rise to an increase in transient energy growth. Nevertheless, we believe that the simple two-degrees-of-freedom models presented in this article capture the essential characteristics of this phenomenon.

Three classical applications have been considered, and it has been demonstrated that significant amplification of energy before the onset of coupled-mode flutter can occur. Whereas panel-flutter and follower-force computations showed substantial short-term energy growth, the transient amplification of initial perturbation was less marked in the case of a fluid-conveying pipe which can be attributed to the flow-induced damping present in the dynamics of the pipe.

As initial perturbations are amplified, nonlinear effects will come into play, and a marked deviation from linear behavior should be expected. Despite this effect, the underlying linear amplification process constitutes an important component in describing the onset of flutter instabilities. For extensions of dynamical systems that exhibit transient growth into the nonlinear regime the interested reader is referred to [13] and references therein.

The transient amplification of initial energy cannot be captured by analyzing the eigenvalues of the system matrix. Instead, both eigenvalues and eigenvectors are needed to account for short-term instabilities. Since these type of instabilities are present before the onset of flutter and show amplification rates of one to two orders of magnitude, nonlinear finite-amplitude effects may be triggered long before the system exhibits vibrational instabilities. When designing fluid-structure systems, an analysis of the type introduced in this paper is recommended.

Acknowledgments

PS wishes to thank Patrick Huerre and the gentle people at LadHyX for making his sabbatical visit so enjoyable.

References

- [1] Butler, K. M., and Farrell, B. F., 1992, "Three-Dimensional Optimal Perturbations in Viscous Shear Flow," *Phys. Fluids A*, **4**, pp. 1637–1650.
- [2] Reddy, S. C., and Henningson, D. S., 1993, "Energy Growth in Viscous Channel Flows," *J. Fluid Mech.*, **252**, pp. 209–238.
- [3] Trefethen, L. N., Trefethen, A. E., Reddy, S. C., and Driscoll, T. A., 1993, "Hydrodynamic Stability Without Eigenvalues," *Science*, **261**, pp. 578–584.
- [4] Schmid, P. J., and Henningson, D. S., 2001, *Stability and Transition in Shear Flows*, Springer-Verlag, New York.
- [5] Dowell, E. H., 1995, *A Modern Course in Aeroelasticity* 3rd Ed., Kluwer, Dordrecht, The Netherlands.
- [6] Bamberger, Y., 1981, *Mechanique de l'Ingenieur. Vol. I. Systèmes de Corps Rigides*, Hermann, Paris.
- [7] Benjamin, B. T., 1961, "Dynamics of a System of Articulated Pipes Conveying Fluids I. Theory," *Proc. R. Soc. London, Ser. A*, **261**, pp. 457–486.
- [8] Blevins, R. D., 1991, *Flow-Induced Vibration*, 2nd Ed., Van Nostrand Reinhold, New York.
- [9] Naudascher, E., and Rockwell, D., 1994, *Flow-Induced Vibrations: An Engineering Guide*, A. A. Balkema, Rotterdam.
- [10] Bolotin, V. V., 1963, *Nonconservative Problems of the Theory of Elastic Stability*, Pergamon Press, New York.
- [11] Semler, C., Alighabari, H., and Païdoussis, M. P., 1998, "A Physical Explanation of the Destabilizing Effect of Damping," *ASME J. Appl. Mech.*, **65**, pp. 642–648.
- [12] Païdoussis, M. P., 1998, *Fluid Structure Interactions. Slender Structures and Axial Flow*, Vol. I, Academic Press, San Diego, CA.
- [13] Gebhardt, T., and Grossmann, S., 1994, "Chaos Transition Despite Linear Stability," *Phys. Rev. E*, **50**, pp. 3705–3711.